Band Limited Signals Observed Over Finite Spatial and Temporal Windows: An Upper Bound to Signal Degrees of Freedom

Farhana Bashar, S.M. Akramus Salehin and Thushara D. Abhayapala
Research School of Engineering
The Australian National University (ANU)
Canberra 0200 ACT, Australia
{farhana.bashar,akramus.salehin,thushara.abhayapala}@anu.edu.au

arXiv:1405.2163v1 [cs.IT] 9 May 2014

Abstract

The study of degrees of freedom of signals observed within spatially diverse broadband multipath fields is an area of ongoing investigation and has a wide range of applications, including characterising broadband MIMO and cooperative networks. However, a fundamental question arises: given a size limitation on the observation region, what is the upper bound on the degrees of freedom of signals observed within a broadband multipath field over a finite time window? In order to address this question, we characterize the multipath field as a sum of a finite number of orthogonal waveforms or spatial modes. We show that (i) the "effective observation time" is independent of spatial modes and different from actual observation time, (ii) in wideband transmission regimes, the "effective bandwidth" is spatial mode dependent and varies from the given frequency bandwidth. These findings clearly indicate the strong coupling between space and time as well as space and frequency in spatially diverse wideband multipath fields. As a result, signal degrees of freedom does not agree with the well-established degrees of freedom result as a product of spatial degrees of freedom and time-frequency degrees of freedom. Instead, analogous to Shannon's communication model where signals are encoded in only one spatial mode, the available signal degrees of freedom in spatially diverse wideband multipath fields is the *time-bandwidth* product result extended from one spatial mode to finite modes. We also show that the degrees of freedom is affected by the acceptable signal to noise ratio (SNR) in each spatial mode.

Index Terms

Degrees of freedom, multipath propagation, spatial sampling, broadband MIMO networks, distributed MIMO.

I. Introduction

A. Motivation and Background

In wireless communications, information is transmitted in the form of waves and space is considered as the physical medium for information transfer. Hence, as a physical process, waves propagate in space via line of sight or multiple paths due to reflection, diffraction and scattering by objects present in the physical environment. Like any other physical phenomenon, wave propagation is governed by the laws of physics. These laws determine the process itself as well as the amount of diversity waves carry along their path. The spatial diversity of multipath influences the amount of information that can be communicated through wave propagation, thus, using spatial diversity of multipath we can ensure better system performances, including capacity improvement, high transmission rate, improved bit error rate etc., [1], [2]. In effect, the study of the spatial degrees of freedom of different multiple antenna systems (i.e., multi-user MIMO systems, distributed MIMO systems, MIMO cognitive radio systems etc.) has gained renewed attention and has more recently been addressed by [3]–[5]. This motivates to study the fundamental limits that space imposes on the degrees of freedom of band limited signals observed over finite spatial and temporal windows.

In this paper, our aim is to determine the upper limit to the degrees of freedom of signals available in a band limited multipath wavefield when the wavefield is observed in, or coupled to a limited source-free region of space over a finite time window. We may assume that multiple antennas or sensors are located in the region of space to sample the observable multipath field for signal processing or communication purposes. We, however, aim to find an upper bound on the available degrees of freedom without explicitly considering a specific propagation condition, physical setup or application and thus, to show that the coupling of time and band limited multipath signals into a spatial region is fundamentally limited by a finite number of spatial modes. Throughout the paper, we will frequently refer to the radius/ size of the $3D$ multipath observation region[1]. Our derived result has great significance in a wide range of applications, including (i) measuring the number of receive antennas required to sample a given region to maximize the performance gain, (ii) characterizing broadband beamforming techniques for next generation wireless

[1]In antenna propagation and sensor array signal processing applications, an alternative terminology is the effective antenna aperture.

communication to provide high quality video and audio, (iii) developing interference alignment scheme for MIMO wireless networks, (iv) characterizing the degrees of freedom of distributed multi-antenna communications for broadband transmissions.

We review the degrees of freedom available in spatially diverse multipath fields in different contexts. Earlier works, [6], [7] focused on multipath fields that exhibit rich scattering and there are independent fading paths between transmitter and receiver antenna elements. According to these works, available degrees of freedom is the minimum number of transmit and receive antenna elements and channel capacity can be improvement remarkably by increasing number of the antenna elements. However, insufficient antenna spacing violates the assumption of independent fading and prevent channel capacity to increase linearly with degrees of freedom [8]. The impact of fading correlation on spatially diverse multipath fields was studied by a large number of research works (e.g., [9], [10]). Afterwards, independent works [11]–[13] provided the characterization of the spatial degrees of freedom in multi-antenna systems as a function of the area, geometry of the antenna arrays and the angular spread of the physical environment. In addition, [14], [15] estimated the degrees of freedom available in source-free narrowband multipath fields observed over a spatial window and showed that the available degrees of freedom scales with the spatial dimension in terms of wavelengths. In contrast, Poon et al. [16] and Franceschetti [17] applied antenna theory and Slepian's theory of spectral concentration, respectively, to derive a fundamental limit on the degrees of freedom available in a wideband multi-antenna systems for a given constraint on the area of the spatial region and observation time and defined the degrees of freedom as a product of spatial degrees of freedom and degrees of freedom of the wideband channel itself. Since for wideband transmissions, space time, and frequency are strongly coupled, available bandwidth and observation time over space respectively differ from actual bandwidth and observation time depending on the available spatial information, the works of [16], [17] did not take this into account. In another approach, [18] characterized multi-antenna systems in a wideband transmission regime and stated that in case of wideband frequency transmission, space and time are strongly coupled. However, how information is conserved in space-time was left as an open and important problem.

B. Our Approach and Contributions

The analysis in this paper considers a wideband multipath wavefield observed within a limited source-free region of space over a finite time window. The signals observable within this wavefield are studied as solutions to the Helmholtz wave equation [19] and they are encoded in infinite but countable number of orthogonal waveforms or spatial modes. This mathematical framework is similarly used in [20], [21].

However, in comparison, our derived result is more accurate, since we have considered the affect of available spatial information not only on the frequency bandwidth but also on the observation time. Further, the degrees of freedom result provided in [20], [21] is derived by using a complex geometrical argument to extend the narrowband degrees of freedom result of [14] to a broadband scenario and resulted in a loose bound. Further, it is unclear, for different spatial modes, how the usable (effective) bandwidth varies from the given frequency bandwidth. In this work, on the contrary, the degrees of freedom result is derived in a simple manner. Moreover, we clarify that at each spatial mode, how (and why) the observable signals are band limited within an effective frequency bandwidth rather than the given frequency bandwidth. In addition, we illustrate that beyond a certain spatial mode, the effective bandwidth becomes zero which in turn, truncates the wavefield from its infinite representation to a finite number of spatial modes. Afterwards, by counting the number of spatial modes required to represent any signal within the given multipath field, we derive an analytical expression to determine the degrees of freedom of the signal[2].

We depict the strong coupling relation between space and time as well as space and frequency in spatially diverse wideband multipath fields. We show that the effective observation time is fixed, independent of spatial modes, different from given observation time and essentially related to the spatial dimension of the observable region. Whereas, for broadband transmissions, at each spatial mode, the observable signal is band limited within an effective frequency bandwidth, since even though the usable bandwidth at the lower spatial modes is equal to the given frequency bandwidth, for the higher modes, the usable bandwidth is less than the given frequency bandwidth. The coupling relations also indicate that for spatially diverse wideband multipath fields, the classical degrees of freedom result of *time-bandwidth product* can not be extended directly to the product of spatial degrees of freedom and *time-bandwidth product* as shown in [16], [17], rather the degrees of freedom result should portray how the time and band limited signals are coupled to a limited region of space. Our derived degrees of freedom result evidently portrays the impact of the coupling relations on the available degrees of freedom in spatially diverse wideband multipath fields. We also show the affect of the acceptable signal to noise ratio (SNR) on the available degrees of freedom of each spatial mode .

[2]A preliminary study for the degrees of freedom were presented previously in [22] and [23], respectively, for $2D$ wavefields and $3D$ wavefields.

C. Organization

The reminder of the paper is organized as follows. In Section II, the problem statement together with background on Shannon's time-frequency degrees of freedom and the eigenbasis expansion of the wavefield are discussed. In Section III, we present our main results, while, Section IV provides graphical analysis of our derived results. Next, Section V elaborates the physical insights of the main results and briefly discusses the applications. We summarize the main contributions of this paper in Section VI.

II. Problem Statement and Background

A. Physical Problem

In this paper, we consider a multipath field band limited to $[F_0 - W, F_0 + W]$ and observed over a time window $[0, T]$ within a $3D$ spatial window enclosed by a spherical region of radius R. Here, F_0 represents the mid band frequency. Any signal sampled or recorded within this spatial region can be expressed as a function of space and time whose spectra lies within the frequency range and whose time function lies within the time interval. Since it is not possible to confine any waveform in both time and frequency, we consider that the spectrum is confined entirely within the frequency range and the time function is negligible outside the time interval.

We now express the space-time signal as

$$\psi(\boldsymbol{x}, t) = \frac{1}{2\pi} \int_{-\infty}^{\infty} \Psi(\boldsymbol{x}, \omega) e^{j\omega t} d\omega \tag{1}$$

where $\Psi(\boldsymbol{x}, \omega)$ is the Fourier transform of $\psi(\boldsymbol{x}, t)$ with respect to t, $\boldsymbol{x}$ represents a position in 3D space, such that $r = \|\boldsymbol{x}\| \leq R$ denotes the euclidean distance of $\boldsymbol{x}$ from the origin, which is the center of the region of interest and $j = \sqrt{-1}$. Due to the band limitedness, $\Psi(\boldsymbol{x}, \omega)$ is assumed to be zero outside the band $[F_0 - W, F_0 + W]$. Thus, the space-time signal can be rewritten as

$$\psi(\boldsymbol{x}, t) = \frac{1}{2\pi} \int_{2\pi(F_0 - W)}^{2\pi(F_0 + W)} \Psi(\boldsymbol{x}, \omega) e^{j\omega t} d\omega. \tag{2}$$

In this work, we aim to answer the fundamental question: *Given constraints on the size of the observation region, frequency bandwidth and observation time window, what is the upper bound on the degrees of freedom of signals observable within multipath wireless fields?*

We will utilize Shannon's result [24] that provides the degrees of freedom of temporal signals for band limited communications over a single channel. Shannon's result states that if the transmission is band limited to $[-W, W]$ and limited to the time interval $[0, T]$, the available time-frequency degrees of freedom is limited to $2WT + 1$. We provide more detailed reasoning of Shannon's result in the next subsection.

B. Shannon's Time-Bandwidth Product

Let us now review the reasoning behind the time-bandwidth product result [24]. In time domain we have a wideband signal and in frequency domain this signal can be expressed as a spectrum. The mapping between these two domains is the Fourier transform. The spectrum is then expanded over the frequency range with the help of Fourier series expansion. This expansion represents the time domain signal by a weighted sum of orthogonal basis functions. Given the signal is approximately time limited to $[0, T]$ and its spectrum is band limited to $[-W, W]$, the minimum number of terms required in the sum to satisfy both of these constraints provide the available degrees of freedom of the signal, $2WT + 1$. Note that there may be slight discrepancy as the time domain signal obtained by the Fourier series expansion over the time interval will not be strictly limited within the frequency band, rather it may contain some frequency component outside the band. However, in another approach, [25]–[28] argued that roughly $2WT + 1$ samples are enough to approximate any signal in energy for the best choice of a complete set of band limited functions which possess the property of being orthogonal over a given finite time interval. Afterwards, the time-bandwidth product result was formalized by several authors [29]–[31] for various other configurations.

However, Shannon's result only accounts for broadband transmission over a single channel. In multipath wireless fields sampled over a region of space, spatial diversity is exploited, for instance, in MIMO communications, providing several independent channels over which information can be transmitted. To account for the spatial diversity of wireless fields, we start with the spherical harmonics analysis of the wavefield observed within a region of space.

C. Spherical Harmonics Analysis of Wavefields

We consider the space-frequency spectrum $\Psi(\boldsymbol{x}, \omega)$ in (2) as a scalar wavefield observed within a $3D$ spherical region of finite radius R generated by a source or distribution of sources and scatterers that exist outside the region of interest at some radius $R_s > R$. Hence, $\Psi(\boldsymbol{x}, \omega)$ satisfies the Helmholtz wave equation (in the region of interest) [32]

$$\nabla^2 \Psi(\boldsymbol{x}, \omega) + k^2 \Psi(\boldsymbol{x}, \omega) = 0 \tag{3}$$

where ∇^2 is the Laplacian, $k = \omega/c$ is the scalar wavenumber, c is the wave velocity and ω is the angular frequency which can be expressed in terms of usual frequency f as $\omega = 2\pi f$. Note that even though we only consider scalar waves, our derived results are equally valid for vector waves [33, pp. 166].

In the spherical coordinate system, the wavefield $\Psi(\boldsymbol{x},\omega)$ in (3) can be decomposed into spherical harmonics which form an orthogonal basis set for the representation of the wavefield. Using the Jacobi-Anger expansion [19, pp. 32] and the addition theorem [19, Theorem 2.8], we can express $\Psi(\boldsymbol{x},\omega)$ as follows

$$\Psi(\boldsymbol{x},\omega) = \sum_{n=0}^{\infty}\sum_{m=-n}^{n} \Psi_{nm}(r,\omega)Y_{nm}(\hat{\boldsymbol{x}}) \tag{4}$$

where spatial mode $n(\geq 0)$ and spatial order m ($|m| \leq n$) are integers, such that for any particular mode n, there are $2n+1$ orders, $\hat{\boldsymbol{x}} \triangleq \boldsymbol{x}/\|\boldsymbol{x}\|$ is the unit vector in the direction of nonzero vector $\boldsymbol{x}$, $Y_{nm}(\cdot)$ are the spherical harmonics and $\Psi_{nm}(r,\omega)$ are the harmonic coefficients. These harmonic coefficients can be expressed as the product of the frequency dependent coefficients $\alpha_{nm}(\omega)$ and the spherical Bessel functions of the first kind $j_n(\omega r/c)$ [34, p. 227] as

$$\Psi_{nm}(r,\omega) \triangleq \alpha_{nm}(\omega) j_n\left(\frac{\omega}{c}r\right). \tag{5}$$

Further, we can think of $\Psi_{nm}(r,\omega)$ as the space-frequency spectrum encoded in n modes and m orders. In this work, we frequently refer to $(m,n)^{th}$ mode space-frequency spectrum which represents the spectrum at a particular mode n and order m. On the contrary, n^{th} mode space-frequency spectrum refers to the n^{th} mode spectrum considering all of the $2n+1$ orders.

Note that $\Psi_{nm}(r,\omega)$ depends only on frequency and radial coordinate r of vector $\boldsymbol{x}$, not on angular information of vector $\boldsymbol{x}$. Also note that the spherical harmonics $Y_{nm}(\cdot)$ exhibit the following orthonormal property [34, p. 191]

$$\int_{\Omega} Y_{nm}(\hat{\boldsymbol{x}}) Y^{*}_{\acute{n}\acute{m}}(\hat{\boldsymbol{x}}) d\Omega = \delta_{n\acute{n}}\delta_{m\acute{m}} \tag{6}$$

where the integration is taken over the unit sphere Ω and δ_{nm} is the Kronecker delta function which is defined as $\delta_{nn} = 1$ and $\delta_{nm} = 0$ if $n \neq m$.

The expansion of the wavefield (4) can be viewed as a weighted sum of orthogonal spherical waveforms encoded in an infinite but countable number of spatial modes. This expansion was used in [14], [15] to represent general narrowband multipath fields observed over a region of space. The work of [14], [15] truncated the spherical harmonic expansion of the wavefield to a finite number of spatial modes which contain most of the energy. The number of spatial modes in the truncated expansion indicate the spatial degrees of freedom (i.e., the number of independent channels). Hence, in this work, we need to find a suitable way to truncate this expansion for broadband multipath fields observed over a region of space.

III. Main Results

In this section, we derive an upper bound to the available degrees of freedom of any signal observed within a band limited multipath field over a spherical region of finite radius for a finite time interval. Before proceeding to the main result presented in this work, we can reasonably ask, how the observable time and band limited signals are coupled to a limited region of space for each spatial mode? In order to answer this question, we first show the coupling of time limited signals to a finite spatial window for each spatial mode n.

A. Effective Observation Time of the Spatial Modes

Lets consider the multipath wavefield is generated by a single farfield source transmitting a time domain signal. The wavefield is enclosed within a spherical region of radius R. Hence, time required for the time domain signal to travel across the diameter of the spherical region is $2R/c$. Further, the wavefield is observed over a time window $[0, T]$. As a result, the observable multipath field captures information content of the time domain signal over a time interval $T + 2R/c$. In the following theorem, we formalize this statement for the n^{th} mode space-time wavefield $\psi_{nm}(r, t)$ generated by the n^{th} mode time domain signal $a_{nm}(t)$.

Theorem 1 (Observation time of the spatial Modes): Given a multipath field observed over a spherical region of radius R for a time interval T that is encoded in a countable number of spatial modes n, then it is possible to capture information about the underlying n^{th} mode time domain signal $a_{nm}(t)$ over an effective time interval

$$T_{eff} = T + \frac{2R}{c}. \tag{7}$$

Further, this effective time interval T_{eff} is independent of the spatial mode index n.

Proof of the theorem is provided in Appendix A.

Remarks 1: Observing the n^{th} mode space-time wavefield $\psi_{nm}(r, t)$ over a time window $[0, T]$ within a spatial window $0 \leq r \leq R$ is equivalent to observing the n^{th} mode time domain signal $a_{nm}(t)$ over the time window $[-R/c, T + R/c]$. Hence, the effective time interval is essentially related to the spatial observation region. This indicates the coupling relation between space and time. Further, the effective time interval is fixed and independent of spatial modes n.

In the next subsection, we show the coupling relation between space and frequency. This relation truncates the expansion in (4) to a finite number of spatial modes.

B. Effective Bandwidth of the Spatial Modes

The performance of wireless communication systems is highly determined by noise. Ideally, if the wireless communication systems are noiseless, it would be possible to measure signals with infinite precision and each spatial mode n would have an effective bandwidth equal to the given frequency bandwidth, i.e., from $F_0 - W$ to $F_0 + W$. However, in practical systems, signals are perturbed by noise. Hence, it is not possible to detect signals within the band of frequencies where the signal to noise ratio (SNR) drops below a certain threshold γ. This threshold is dependent on the antenna/ sensor sensitivity or the robustness of the signal processing method to noise.

To determine how noise affects the available bandwidth at each spatial mode n, let us assume that $\eta_R(\hat{\boldsymbol{x}}, \omega)$ is the white Gaussian noise on the surface of the spherical region (at radius R) associated with the antenna/ sensor at the angular position $\hat{\boldsymbol{x}}$. Hence, from (4) and (5), the space-frequency spectrum on the sphere is

$$\Psi(R, \hat{\boldsymbol{x}}, \omega) = \sum_{n=0}^{\infty} \sum_{m=-n}^{n} \alpha_{nm}(\omega) j_n\left(\frac{\omega}{c} r\right) Y_{nm}(\hat{\boldsymbol{x}}) + \eta_R(\hat{\boldsymbol{x}}, \omega). \tag{8}$$

In the following theorem and corollary, we characterize the white Gaussian noise at the different modes.

Theorem 2 (White Gaussian Noise in L^2): Given a zero mean white Gaussian noise with variance σ_0^2 in $L^2(\mathbb{S}^2)$ represented by a random variable $\eta_R(\hat{\boldsymbol{x}})$ where $\hat{\boldsymbol{x}} \in \mathbb{S}^2$, such that for any function $\psi_i(\hat{\boldsymbol{x}}) \in L^2(\mathbb{S}^2)$ the complex scalar

$$\nu_i \triangleq \int_{\mathbb{S}^2} \eta_R(\hat{\boldsymbol{x}}) \psi_i^*(\hat{\boldsymbol{x}}) d\hat{\boldsymbol{x}} = \langle \eta_R(\hat{\boldsymbol{x}}), \psi_i(\hat{\boldsymbol{x}}) \rangle \tag{9}$$

is also a zero mean Gaussian random variable with variance $E\{|\nu_i|^2\} = \sigma_0^2 \int_{\mathbb{S}^2} |\psi_i(\hat{\boldsymbol{x}})|^2 d\hat{\boldsymbol{x}} = \sigma_0^2 (\|\psi_i(\hat{\boldsymbol{x}})\|_{L^2})^2$. [35, eqn 8.1.35]

Corollary 1: Considering $\psi_i(\hat{x})$ to be the orthonormal basis functions $Y_{nm}(\hat{\boldsymbol{x}})$, the spatial Fourier coefficients for the noise is

$$\nu_{nm}(\omega) = \int_{\mathbb{S}^2} \eta_R(\hat{\boldsymbol{x}}, \omega) Y_{nm}^*(\hat{\boldsymbol{x}}) d\hat{\boldsymbol{x}}. \tag{10}$$

Applying Theorem 2, $\nu_{nm}(\omega)$ are also zero mean Gaussian random variables with variance

$$E\{|\nu_{nm}(\omega)|^2\} = \sigma_0^2(\omega) \int_{\mathbb{S}^2} |Y_{nm}^*(\hat{\boldsymbol{x}})|^2 d\hat{\boldsymbol{x}} = \sigma_0^2(\omega) \tag{11}$$

where the noise power is independent of the mode. Further, since the noise is white Gaussian, the noise power is the same at all frequencies ω, i.e.,

$$E\{|\nu_{nm}(\omega)|^2\} = \sigma_0^2. \tag{12}$$

Based on Corollary 1, we can define the $(m,n)^{th}$ mode space-frequency spectrum at radius R as

$$\Psi_{nm}(R,\omega) = \alpha_{nm}(\omega) j_n\left(\frac{\omega}{c}R\right) + \nu_{nm}(\omega) \tag{13}$$

and we assume that the noise and the signal are not dependent on each other. Here, the $(m,n)^{th}$ mode space-frequency spectrum $\Psi_{nm}(R,\omega)$ takes white Gaussian noise $\nu_{nm}(\omega)$ into account. This white Gaussian noise has the property that each spatial mode is perturbed independently of all the others. Further, $\alpha_{nm}(\omega)$ is the $(m,n)^{th}$ mode signal spectrum band limited over the range $[F_0 - W, F_0 + W]$. In contrast, for a fixed value of the radius, $j_n(\omega R/c)$ can be treated as a function of frequency. However, it is evident from Fig. 1 that except for the the 0^{th} order, the spherical Bessel functions $j_n(z)$ start small before increasing monotonically to their maximum. Therefore, for frequencies less than a critical frequency F_n, the magnitude of the n^{th} order spherical Bessel function $|j_n(\omega R/c)|$ is negligible.

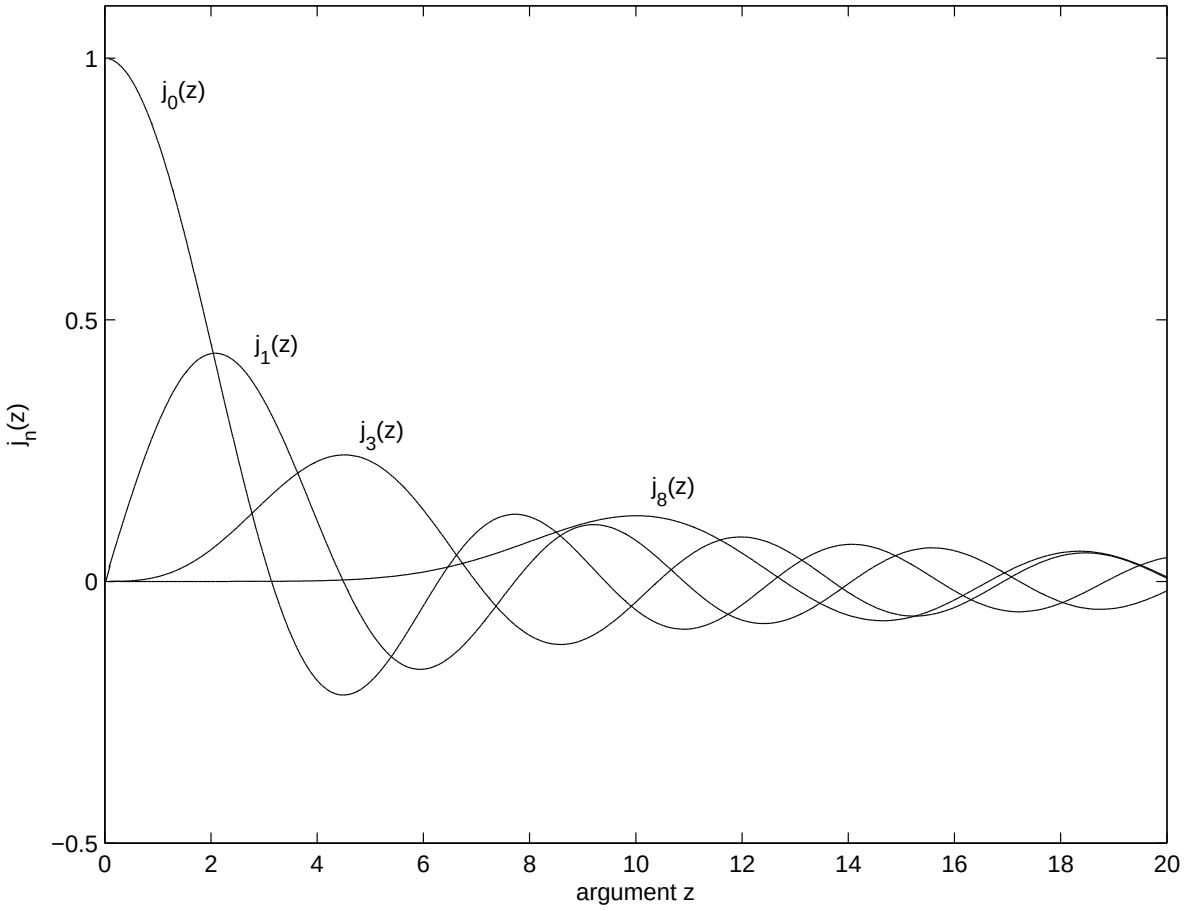

Fig. 1. Spherical Bessel functions of first kind $j_n(z)$ vs. argument z for $n = 0, 1, 3, 8$.

At each spatial mode $n > 0$, for frequencies less than a critical frequency F_n, the SNR is less than the threshold γ. As a result, we can not detect the space-frequency spectrum for frequencies less than F_n. In addition, as depicted in Fig. 1, the spherical Bessel functions $j_n(z)(n > 0)$ start more slowly as n increases. Thus, after a certain spatial mode n, the critical frequency F_n is larger than the lower bound of the given bandwidth $F_0 - W$ and the useable (effective) bandwidth of this mode and the modes above varies from the given frequency bandwidth. The following theorem provides the effective bandwidth available at each spatial mode n.

Theorem 3 (Effective Bandwidth of the n^{th} Mode): Any wireless multipath wavefield observed within a spherical region of space bounded by radius R over a frequency range $[F_0 - W, F_0 + W]$ is encoded in a finite number of spatial modes $0 \le n \le N_{\max}$ where the effective frequency bandwidth of the n^{th} mode space-frequency spectrum $\Psi_{nm}(R, \omega)$ is

$$W_n = \begin{cases} 2W, & 0 \le n \le N_{\min} \\ F_0 + W - F_n, & N_{\min} < n \le N_{\max} \\ 0, & \text{otherwise.} \end{cases} \tag{14}$$

Here, $N_{\min}$ is the lowest spatial mode beyond which the critical frequency $F_n > F_0 - W$, $N_{\max}$ is the lowest spatial mode beyond which the critical frequency $F_n > F_0 + W$ and

$$F_n = \frac{nc}{e\pi R} + \frac{c}{2e\pi R} \log\left(\frac{\gamma}{(SNR)_{\alpha,\max}}\right) \tag{15}$$

with the threshold γ depicting the ability of the system to detect signals buried in noise. Further, we consider that the power of the n^{th} mode signal spectrum $\alpha_{nm}(\omega)$ is finite and bounded for all modes n, orders m and frequencies ω, i.e.,

$$E\{|\alpha_{nm}(\omega)|^2\} \le |\alpha_{\max}|^2, \quad \forall n, m, \omega \tag{16}$$

hence, the maximum SNR of the signal spectrum $\alpha_{nm}(\omega)$ for any mode n is

$$(SNR)_{\alpha,\max} = \frac{|\alpha_{\max}|^2}{\sigma_0^2}. \tag{17}$$

Proof of the theorem is given in Appendix B.

Remarks 2: The effective frequency bandwidth of each spatial mode is related to the spatial observation region and varies from the given frequency bandwidth depending on the critical frequency F_n. This portrays the strong coupling relation between space and frequency. Further, for $n > N_{\max}$, the critical

frequency F_n is greater than the upper bound of the given frequency range $F_0 + W$. Therefore, we can truncate the expansion in (4) to a finite number of spatial modes as

$$\Psi(\boldsymbol{x}, \omega) = \sum_{n=0}^{N_{\max}} \sum_{m=-n}^{n} \Psi_{nm}(r, \omega) Y_{nm}(\hat{\boldsymbol{x}}). \tag{18}$$

Using (15), the upper bound for the spatial modes $N_{\max}$ is

$$N_{\max} = \left\lceil e\pi(F_0 + W)\frac{R}{c} + \frac{1}{2}\log\left(\frac{(SNR)_{\alpha,\max}}{\gamma}\right)\right\rceil \tag{19}$$

where $\lceil \cdot \rceil$ is the ceiling value, since by definition spatial modes are integers.

C. Upper Bound to Signal Degrees of Freedom

We are now in a position to provide an upper bound to the available degrees of freedom of wideband signals observed over finite spatial and temporal windows. In order to do so, it is useful to think of $(m, n)^{th}$ mode space-frequency spectrum $\Psi_{nm}(r, \omega)$ in time domain, in which case we obtain

$$\psi_{nm}(r, t) = \frac{1}{2\pi}\int_{\Omega_n} \Psi_{nm}(r, \omega) e^{j\omega t} d\omega \tag{20}$$

where $\psi_{nm}(r, t)$ is the inverse Fourier transform of $\Psi_{nm}(r, \omega)$ with respect to ω and the integration is taken over Ω_n with $\Omega_n \in [2\pi(F_0 - W), 2\pi(F_0 + W)]$ for $0 \le n \le N_{\min}$ and $\Omega_n \in [2\pi F_n, 2\pi(F_0 + W)]$ for $N_{\min} < n \le N_{\max}$ where F_n is defined in (15).

We expand $\Psi_{nm}(r, \omega)$ over the frequency range using the Fourier series expansion, similar to [24], as follows

$$\Psi_{nm}(r, \omega) = \sum_{\ell=-\infty}^{\infty} c_{nm\ell}(r) e^{-j\omega\frac{\ell}{W_n}} \tag{21}$$

where the Fourier coefficients

$$\begin{aligned} c_{nm\ell}(r) &= \frac{1}{2\pi W_n}\int_{\Omega_n} \Psi_{nm}(r, \omega) e^{j\omega\frac{\ell}{W_n}} d\omega \\ &= \frac{1}{W_n}\psi_{nm}(r, \frac{\ell}{W_n}) \end{aligned} \tag{22}$$

are proportional to the samples of $\psi_{nm}(r, t)$ and W_n is the effective frequency of the n^{th} mode defined in (14). The result (22) is obtained from (20) when $t = \ell/W_n$. It illustrates that the samples of $\psi_{nm}(r, t)$ determine the coefficients $c_{nm\ell}(r)$ in the Fourier series expansion. Therefore, analogous to Shannon's work [24], we can reconstruct the $(m, n)^{th}$ mode space-time signal $\psi_{nm}(r, t)$ from its samples as follows

$$\psi_{nm}(r, t) = \sum_{\ell=-\infty}^{\infty} \psi_{nm}(r, \frac{\ell}{W_n}) e^{j2\pi W_{0n}(t-\frac{\ell}{W_n})} \frac{\sin \pi W_n(t - \frac{\ell}{W_n})}{\pi W_n(t - \frac{\ell}{W_n})} \tag{23}$$

where W_{0n} is the mid band frequency of the $(m,n)^{th}$ mode. We obtain (23) by substituting the Fourier series (21) in (20), applying (22) and then exchanging integration and summation.

Hence, it is possible to reconstruct the space-time signal $\psi(\boldsymbol{x},t)$ (2) by summing the $(m,n)^{th}$ mode space-time signals for all possible values of n and m over all propagation directions, i.e.,

$$\psi(\boldsymbol{x},t) = \sum_{n=0}^{N_{\max}} \sum_{m=-n}^{n} \psi_{nm}(r,t) Y_{nm}(\hat{\boldsymbol{x}}) \tag{24}$$

and substituting (23) yields

$$\psi(\boldsymbol{x},t) = \sum_{n=0}^{N_{\max}} \sum_{m=-n}^{n} \sum_{\ell=-\infty}^{\infty} \psi_{nm}\left(r, \frac{\ell}{W_n}\right) e^{j2\pi W_{0n}(t-\frac{\ell}{W_n})} \frac{\sin \pi W_n (t-\frac{\ell}{W_n})}{\pi W_n (t-\frac{\ell}{W_n})} Y_{nm}(\hat{\boldsymbol{x}}). \tag{25}$$

Observe that the spherical harmonics $Y_{nm}(\hat{\boldsymbol{x}})$ are orthogonal over the spherical region as shown in (6). Further, considering

$$\phi_\ell(t) = e^{j2\pi W_{0n}(t-\frac{\ell}{W_n})} \frac{\sin \pi W_n (t-\frac{\ell}{W_n})}{\pi W_n (t-\frac{\ell}{W_n})}, \tag{26}$$

the functions $\phi_\ell(t)$ are orthogonal over time. Proof of the orthogonality of the functions $\phi_\ell(t)$ is provided in Appendix C. Therefore, following the same reasoning as Shannon [24], discussed in Section II-B, the minimum numbers of terms required in the sum (25) that satisfy the constraints on observation region size, bandwidth and observation time window provide the available signal degrees of freedom within the given multipath field. Here, ℓ can be truncated to $[0, W_n T_{eff}]$. We truncate ℓ based on the fact that the $(m,n)^{th}$ mode space-time signal $\psi_{nm}(r,t)$ (23) is band limited to W_n. Hence, we can determine $\psi_{nm}(r,t)$ by taking samples $1/W_n$ units apart. Now, in order to limit $\psi_{nm}(r,t)$ within the interval T_{eff}, $\psi_{nm}(r,\ell/W_n)$ is non-zero for only the appropriate values of ℓ, such that $0 \leq \ell \leq W_n T_{eff}$. This means that the degrees of freedom of the $(m,n)^{th}$ mode space-time signal $\psi_{nm}(r,t)$ is $1 + W_n T_{eff}$. Hence, the total degrees of freedom of any signal available in the given multipath field considering all modes and orders is given by

$$D = \sum_{n=0}^{N_{max}} \sum_{m=-n}^{n} (W_n T_{eff} + 1) \tag{27}$$

where for different values of n, W_n is provided in (14) and T_{eff} is defined in (7).

Using our previous results, we now provide the following theorem for the degrees of freedom of any signal observed within a broadband multipath field.

Theorem 4: Given a multipath wireless field band limited to $[F_0 - W, F_0 + W]$ over the time interval $[0,T]$ within a $3D$ spherical region of radius R, then the degrees of freedom of any signal observable

within this multipath field is upper bounded by

$$D \leq (N_{\max}+1)^2 + 2W\left(T+\frac{2R}{c}\right)\Big[(N_{\min}+1)^2 + 2\left(e\pi\frac{R}{c}\right)^2\left(F_0W-\frac{1}{3}W^2\right) + e\pi\frac{R}{c}(2F_0-W) + \log\left(\frac{(SNR)_{\alpha,\max}}{\gamma}\right)\left(e\pi W\frac{R}{c}+1\right)\Big] \tag{28}$$

where $N_{\max}$ is defined in (19) and from Theorem 3, $N_{\min}$ is the lowest spatial mode beyond which the critical frequency $F_n > F_0 - W$. Using (15),

$$N_{\min} = \left\lceil e\pi(F_0-W)\frac{R}{c} + \frac{1}{2}\log\left(\frac{(SNR)_{\alpha,\max}}{\gamma}\right)\right\rceil. \tag{29}$$

Since by definition spatial modes are integers, $N_{\min}$ is defined as a ceiling value.

Proof of the theorem is given in Appendix D.

In the next section, we graphically illustrate our derived results.

IV. Graphical Illustrations

Consider λ_0 as the wavelength corresponding to the mid band frequency F_0. Therefore, R, W, and T can be represented in terms of λ_0 or F_0 as follows

$$\begin{aligned} R &= a\lambda_0, \quad a \in [0,\infty) \\ W &= bF_0, \quad b \in [0,1] \\ T &= d/F_0, \quad d \in [0,\infty) \end{aligned} \tag{30}$$

where a, b and d are real numbers. Furthermore, $c = F_0\lambda_0$ and $W = F_0$ represents the extreme broadband scenario. Hence, (28) can be rewritten as

$$D \leq (\eta_{\max}+1)^2 \quad + \quad b(2a+d)[2(\eta_{\min}+1)^2 + (2e\pi ab)^2(1/b-1/3) + 2e\pi ab(2/b-1) + 2\log\rho(e\pi ab+1)] \tag{31}$$

where considering $\rho = (SNR)_{\alpha,\max}/\gamma$,

$$\eta_{\max} = N_{\max}(a,b,\rho) = \lceil e\pi a(1+b) + (1/2)\log\rho\rceil$$

and

$$\eta_{\min} = N_{\min}(a,b,\rho) = \lceil e\pi a(1-b) + (1/2)\log\rho\rceil.$$

In Fig. 2, degrees of freedom D in (31) is plotted as a function of radius of the spherical region and fractional bandwidth. It is evident from the figure that for a given observation time window, there is a sub-quadratic growth in available degrees of freedom with increasing region size and bandwidth. Note

that we consider a scenario with a small value of ρ. Increasing ρ (which is equivalent of minimizing the affect of noise) we can achieve higher signal degrees of freedom.

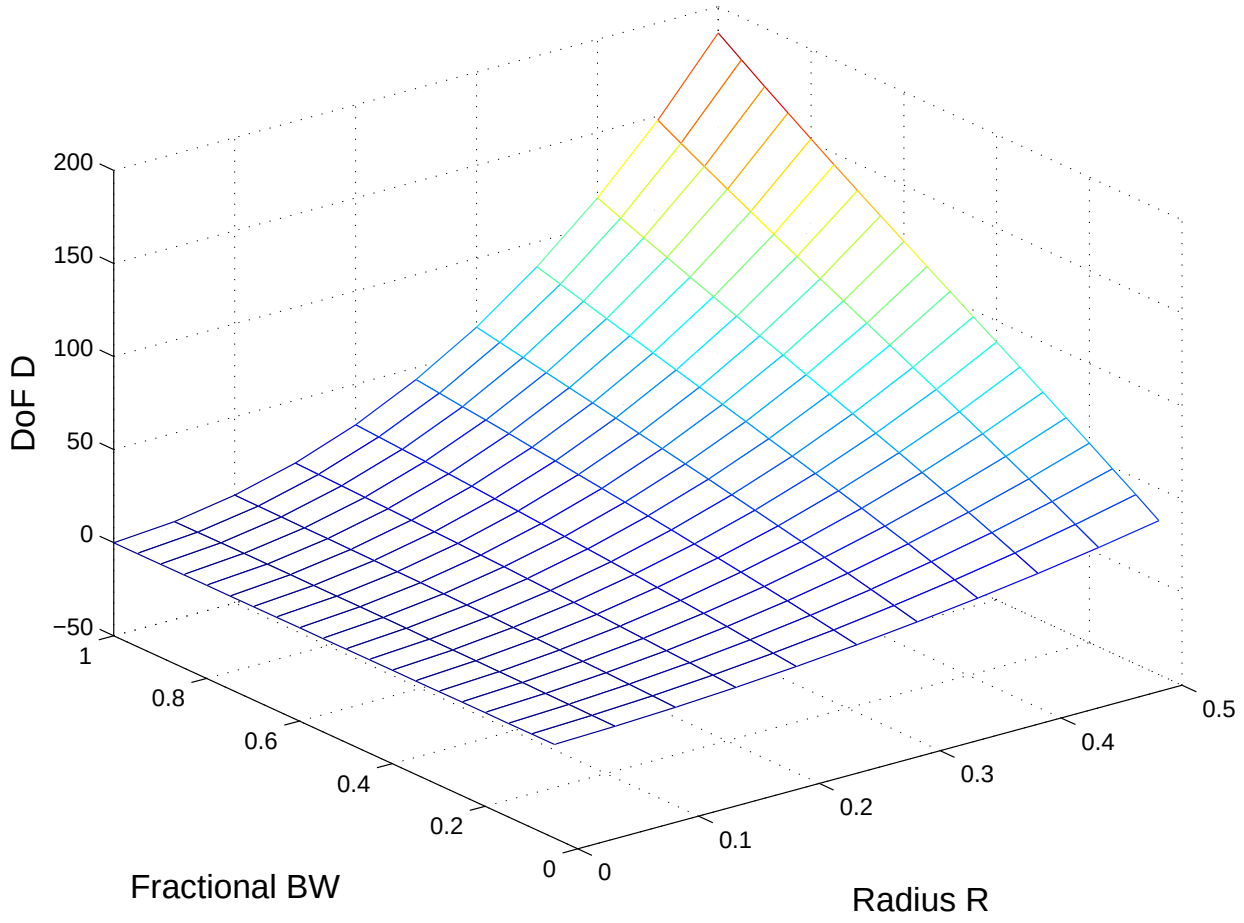

Fig. 2. Degrees of Freedom (DoF) D vs. radius R vs. fractional BW at a fixed observation time window (d = 1) for ρ = .5. Radius, fractional BW and observation time are defined in (30).

Next, we portray the affect of SNR on signal degrees of freedom considering different values of ρ. It is evident from Fig. 3 that for a given observation time window, increasing the value of ρ, we can obtain a growth in degrees of freedom as a function of (a) radius of the observable region and (b) bandwidth, respectively.

We now present the signal degrees of freedom as a function of bandwidth at a fixed observation time window. The parameter is the radius of the observable spherical region with $a = \{0.5, 1, 1.5, 2\}$. The results in Fig. 4 (a) demonstrate that the degrees of freedom increases sub-quadratically as the radius of the observable region increases.

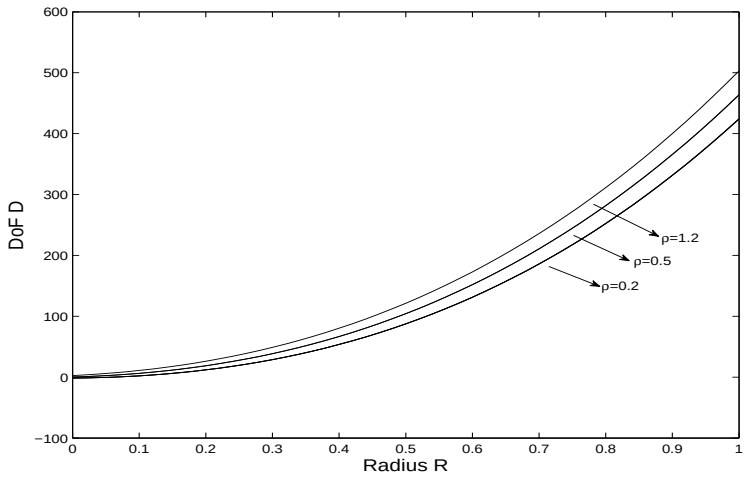

(a) DoF D vs. radius R.

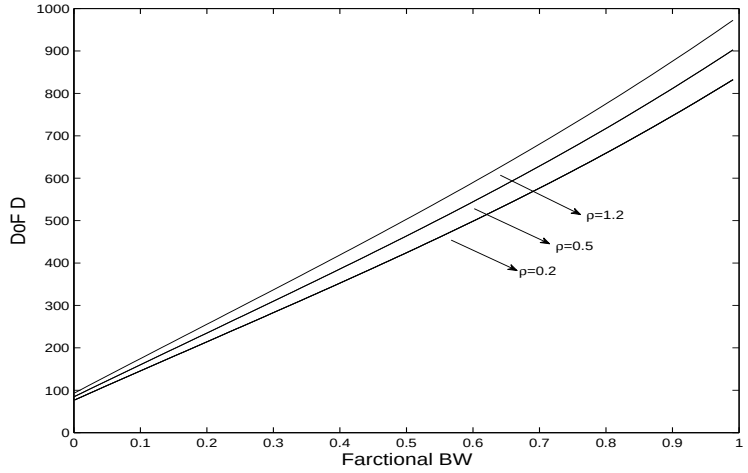

(b) DoF D vs. fractional BW

Fig. 3. Degrees of Freedom for different values of ρ at a fixed time window (d = 1) (a) for a fixed bandwidth (b = 0.5), (b) for a fixed radius of the region (a = 1).

On the contrary, it is clear from Fig. 4 (b) that considering a fixed bandwidth, by increasing the radius of the observable region, it is possible to obtain a rapid non-linear growth in the degrees of freedom as a function of observation time.

Note that the two scenarios mentioned above clearly indicate that we can obtain significantly high signal degrees of freedom only by increasing the radius of the observable region irrespective of bandwidth or

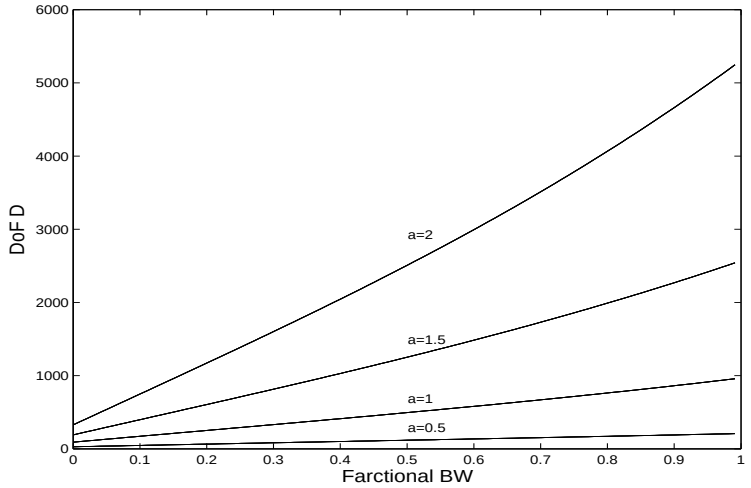

(a) DoF D vs. fractional BW.

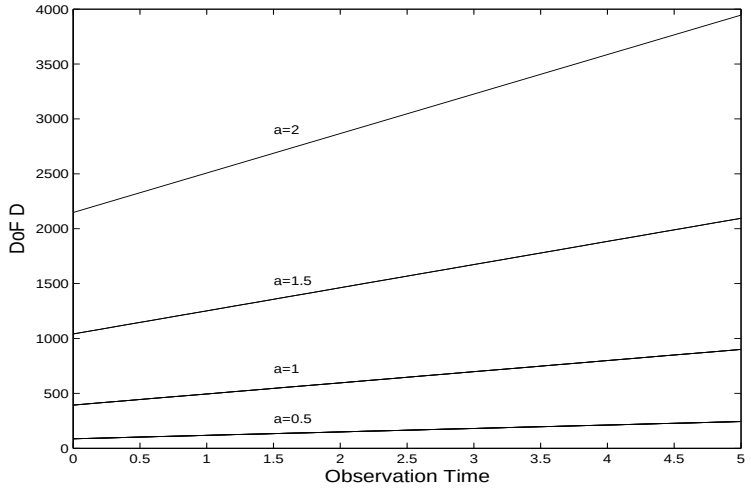

(b) DoF D vs. observation time

Fig. 4. Degrees of Freedom at different radius $R = a\lambda_0$ considering $\rho = 1$ (a) for a fixed time window ($d = 1$), (b) for a fixed bandwidth ($b = 0.5$).

observation time. This significant growth is also true if we increase the bandwidth but keep the radius of the region and observation time constant.

From the results, increasing the frequency or the radius leads to a sub-quadratic growth in the degrees of freedom. On the other hand, increasing the observation time window or the SNR does not provide such a significant increase in the degrees of freedom.

V. DISCUSSION

In this section, we elucidate the physical insights of the main results and attempt to briefly discuss about their applications. We can make the following comments based on Theorem 4:

- From a spatial diversity perspective, in Shannon's proposed communication model [24], wideband signals are encoded in only one spatial mode or one channel over which information is transmitted. On the contrary, our proposed model contains spatially diverse wideband signals that are encoded in a finite number of spatial modes n. As a result, intuitively the available degrees of freedom of any wideband signal observed over finite spatial and temporal windows should be Shannon's degrees of freedom result extended form one spatial mode to n modes. Our derived result clearly comply with this intuition. The number of modes are the number of independent channels available to receive information due to the availability of measurements over a spatial region. This means that each mode or channel has its own time-frequency degrees of freedom. Spatial diversity, therefore, provides a number of independent channels over which time-frequency information can be transmitted.
- The degrees of freedom result does not agree with the well established result of evaluating degrees of freedom of spatially diverse wideband signals as a product of spatial degrees of freedom and time-frequency degrees of freedom [16], [17]. However, in the propagation of waves even though space, time and frequency are separate entities, in spatially diverse wideband transmissions, space and time as well as space and frequency are strongly coupled, the results of [16], [17] fail to show those coupling relationships. On the contrary, our derived result takes the coupling relations in account.
- Shannon's work considers broadband transmission over a single channel and shows that the channel has *'time-bandwidth product +1'* degrees of freedom. On the contrary, in addition to broadband transmission, we take spatial diversity in account. Therefore, in this work, we consider broadband transmission over finite n number of channels. Our analysis indicates that each of these channels has *'effective time-effective bandwidth product +1'* degrees of freedom. This means that considering spatial diversity, we can capture more information from broadband transmission. For higher modes, the effective/ usable bandwidth is less than the measured bandwidth and so not all spatial modes can covey the same amount of information. Therefore, from Theorem 3, for modes n above $N_{\min}$, the *'effective time-effective bandwidth product +1'* decreases as the mode n increases.

A. Asymptotic Results

Let us consider that the threshold is equivalent to the maximum SNR of the n^{th} mode signal spectrum $\alpha_{nm}(\omega)$, i.e., $\gamma = (SNR)_{\alpha,\max}$. This means that signals below the frequency $F_n = nc/(e\pi R)$ are

submerged in noise and can not be detected. As a result, from (28) we obtain

$$D \leq \underbrace{\left(\lceil e\pi(F_0+W)\frac{R}{c}\rceil+1\right)^2}_{D_1} + \underbrace{2W\left(T+\frac{2R}{c}\right)\left(\lceil e\pi(F_0-W)\frac{R}{c}\rceil+1\right)^2}_{D_2} + \underbrace{W\left(T+\frac{2R}{c}\right)\left[\left(2e\pi\frac{R}{c}\right)^2\left(F_0W-\frac{W^2}{3}\right)+2e\pi\frac{R}{c}(2F_0-W)\right]}_{D_3} \tag{32}$$

which yields the following observations:

- For non-spatially diverse multipath fields $(R = 0)$, in (32), D_1 reduces to 1, D_2 reduces to $2WT$ and D_3 becomes zero. Thus, non-spatially diverse multipath fields provide $2WT+1$ degrees of freedom.
- For narrowband wavefields $(W = 0)$, in (32), D_1 reduces to $(\lceil e\pi F_0R/c\rceil+1)^2$, whereas, both D_2 and D_3 become zero. Hence, there are $(\lceil e\pi F_0R/c\rceil+1)^2$ degrees of freedom available in narrowband wavefields operating at the mid band frequency F_0. As a result, in terms of wavelengths, degrees of freedom available in narrowband wavefields is $(\lceil e\pi R/\lambda_0\rceil+1)^2$ where $\lambda_0 = c/F_0$ is the wavelength corresponding to the mid band frequency F_0.
- If any signal observable within a multipath field is representable with only one sample in time domain $(T = 0)$, then, by substituting $T = 0$ in (32), we obtain

$$D \leq \left(\lceil e\pi(F_0+W)\frac{R}{c}\rceil+1\right)^2 + 4W\frac{R}{c}\left(\lceil e\pi(F_0-W)\frac{R}{c}\rceil+1\right)^2 + 2W\frac{R}{c}\left[\left(2e\pi\frac{R}{c}\right)^2\left(F_0W-\frac{W^2}{3}\right)+2e\pi\frac{R}{c}(2F_0-W)\right]. \tag{33}$$

  This equation indicates that even when there is only one sample available in time domain, spatial diversity influences the amount of information that can be captured within the observable region.

The derived result (32) represents the degrees of freedom of signals observable within a broadband multipath field over finite spatial and time windows, assuming the signals are submerged in noise for frequencies less than the critical frequency $F_n = nc/(e\pi R)$ and are not detectable. This result is consistent with Shannon's time-frequency degrees of freedom result [24] when we take sample at a single spatial point $(R = 0)$. Further, (32) is consistent with the degrees of result derived in [15, eqn. 44] at wavelength λ_0 when we consider narrowband frequency transmissions $(W = 0)$.

B. Applications

The degrees of freedom result obtained in this paper can be used to provide insights and bounds in the following areas:

- In the context of spatial broadband communications such as wireless MIMO communications, this work addresses the fundamental question of how the spatial degrees of freedom is interrelated to the time-frequency degrees of freedom. The result provides insights into gains or losses of degrees of freedom in space and time-frequency analysis.
- For broadband beamforming the degrees of freedom characterises the maximum resolution that can be obtained [36]. The greater the degrees of freedom the higher the resolution can be obtained. This has particular importance in this area since we have more variables to work with to perform broadband beamforming. The performance of beamforming in wireless networks improves with the available degrees of freedom and has been shown in [37]. In next generation of wireless communications capable of transmitting high quality video and audio, array gain is obtained by using broadband beamforming which exploits the spatial degrees of freedom and the effective bandwidth of each of these spatial degrees. Our work shows that as more spatial degrees are exploited for beamforming, for a receive antenna occupying a limited spatial region, the effective bandwidth of the higher spatial degrees or modes n are less than the bandwidth and decreases with the mode index n.
- For broadband reception of signals by antennas placed within a given spatial region, initially linear growth in the degrees of freedom is obtained with increasing number of antennas. Once the number of antennas is greater than $(N_{\min}+1)^2$, the increase in degrees of freedom reduces with each antenna added until number of antennas is equivalent to $(N_{\max}+1)^2$. After that no gain can be obtained. This is because the wavefield constraint results in correlations between channels when the number of antennas becomes too large.
- Interference alignment is a promising new area introduced in the last two decades. This seeks to solve the spectrum scarcity in wireless communications by utilizing the available degrees of freedom in space, time and frequency [4], [38]. However, in MIMO wireless networks, interference alignment uses the parallel channels in space offered by spatial degrees of freedom for alignment. Our derived results can be used to develop an interference alignment scheme for MIMO wireless networks. Our results show that optimal signal alignment needs to consider that not all spatial channels are equal and can place interference on the spatial channels that have the lower time-frequency degrees of freedom. Hence, the interference channels should be placed in the spatial channels corresponding to the higher spatial modes. Further, the degrees of freedom analysis of this work provides the maximum degrees of freedom that can be utilized in these broadband communications with interference.
- Recently, distributed MIMO communications have seen an increase in importance due to the popularity of sensor and ad-hoc networks. Distributed MIMO includes all muti-user communication

configurations where the communications input and outputs are distributed over different users. Works of [5], [39], [40] have studied the spatial degrees of freedom for these considering different channel conditions and showed performance gains. These works looked at only narrowband transmissions, however, practical wireless transmissions are performed over a bandwidth. Considering this, our work shows the maximum degrees of freedom available over space, time and frequency for users in a limited spherical region cooperating to receive broadband information. Also, we show how the time-frequency degrees of freedom is distributed over the spatial modes.

VI. Conclusion

This paper provides an upper bound to the degrees of freedom of any signal observed within a band limited multipath wireless field over finite spatial and temporal windows. This upper bound is obtained characterizing the multipath field as solution to Helmholtz wave equation encoded in a finite number of spatial modes. The analysis of the work shows that the effective observation time is independent of spatial modes and related to the spatial dimension of the observable region. Further, for broadband transmissions, at each spatial mode, the observable signals are band limited within an effective frequency bandwidth and depending on the mode, the effective bandwidth varies from the given frequency bandwidth. These findings imply that when both spatial diversity and broadband transmissions are taken in account, space and time as well as space and frequency cannot be decoupled.

The degrees of freedom result derived in this work takes the coupling relations into account and portrays the interrelation between spatial degrees of freedom and time-frequency degrees of freedom. From a spatial diversity perspective, Shannon's proposed communication model considers wideband signal encoded in only one spatial mode or one channel over which information is transmitted, the available degrees of freedom of spatially diverse wideband signal encoded in finite number of spatial modes n is Shannon's degrees of freedom result extended form one spatial mode to n modes. This means that each mode or channel has its own time-frequency degrees of freedom.

We also show that analogous to time, space can be treated as an information bearing object, since degrees of freedom increases sub-quadratically as the size of the observable spatial region increases irrespective of bandwidth or time window. Further, the derived result portrays how the degrees of freedom is affected by the acceptable SNR at each spatial mode.

APPENDIX A
PROOF OF THEOREM 1

Proof: Let $\psi_{nm}(r,t)$ be the inverse Fourier transform of $\Psi_{nm}(r,\omega)$, then, the inverse Fourier transform of (5) is

$$\psi_{nm}(r,t) = a_{nm}(t) * P_n(\frac{tc}{r}) \tag{34}$$

where the time domain coefficients $a_{nm}(t)$ are the inverse Fourier transform of $\alpha_{nm}(\omega)$ and the Legendre polynomials $P_n(tc/r)$ are the inverse Fourier transform of $j_n(\omega r/c)$.

In (34), we can consider $a_{mn}(t)$ as the n^{th} mode time domain signal. Therefore, the n^{th} mode space-time signal $\psi_{mn}(r,t)$ is a convolution between the n^{th} mode time domain signal $a_{mn}(t)$ with the Legendre polynomial $P_n(tc/r)$. The convolution with the Legendre polynomial $P_n(tc/r)$ represents the wavefield constraint and information content in the n^{th} mode space-time signal $\psi_{mn}(r,t)$ is contained in $a_{mn}(t)$. Further, from the definition in [19, p. 23], Legendre polynomials $P_n(tc/r)$ are defined only for $-r/c \leq t \leq r/c$. This characteristic of Legendre polynomials is also evident from Fig. 5.

We observe the n^{th} mode space-time signal $\psi_{nm}(r,t)$ over a time window $[0,T]$ within a spatial window $0 \leq r \leq R$. Therefore, for the given wavefield constraint, at any particular radius r, we can observe information in the the n^{th} mode time domain signal $a_{mn}(t)$ over the time window $[-r/c, T+r/c]$. If we consider that the n^{th} mode space-time signal is observed within a sphere of radius R, it is possible to capture information about the n^{th} mode time domain signal $a_{nm}(t)$ over a maximum of $T+2R/c$ time interval. Hence, observing the n^{th} mode space-time signal $\psi_{nm}(r,t)$ within a spherical region of radius R over the time window $[0,T]$ is equivalent to observing the n^{th} mode time domain signal $a_{nm}(t)$ over a maximum time window $[-R/c, T+R/c]$. ■

APPENDIX B
PROOF OF THEOREM 3

Proof: Observable multipath field on the surface of the sphere (at radius R) is

$$\Psi(R,\hat{\boldsymbol{x}},\omega) = \sum_{n=0}^{\infty}\sum_{m=-n}^{n} \Psi_{nm}(R,\omega)Y_{nm}(\hat{\boldsymbol{x}}) \tag{35}$$

Applying Parserval's theorem with respect to the spherical harmonics[3], the average power of the observable multipath field from all propagation directions is a sum over the average power in the different

[3]Since the spherical harmonics are independent of each other, we can encode each mode with independent signal spectrums to achieve the maximum degrees of freedom observed in the region.

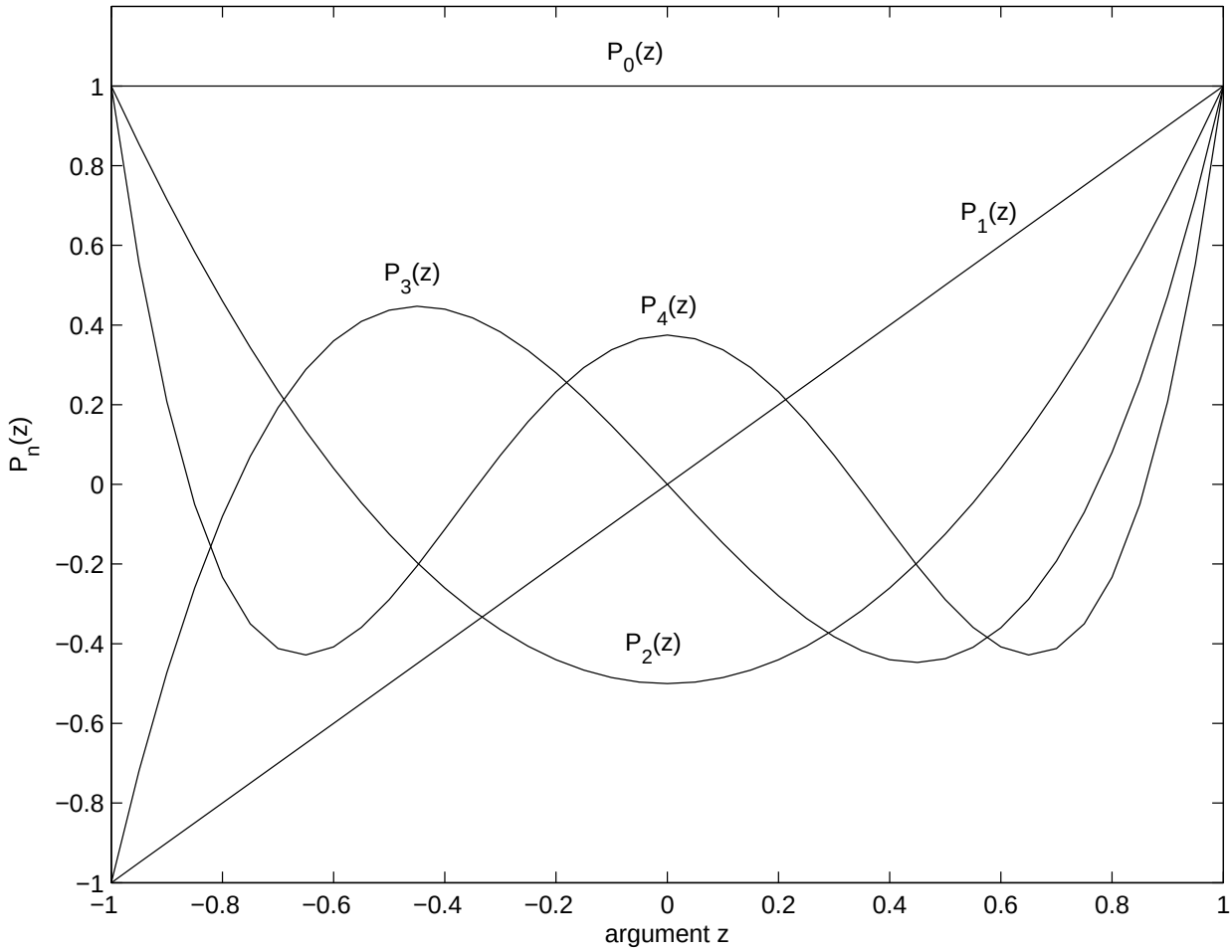

Fig. 5. Legendre Polynomials $P_n(z)$ for $n = 0, 1, 2, 3, 4$.

modes, such that

$$\int_{\mathbb{S}^2} E\{|\Psi(R,\hat{\boldsymbol{x}},\omega)|^2\} d\hat{\boldsymbol{x}} = \sum_{n=0}^{\infty} \sum_{m=-n}^{n} E\{|\Psi_{nm}(R,\omega)|^2\}. \tag{36}$$

Since the noise is independent of the signal, using (13) we obtain

$$E\{|\Psi_{nm}(R,\omega)|^2\} = E\{|\alpha_{nm}(\omega)|^2\} |j_n\left(\frac{\omega}{c}R\right)|^2 + E\{|\nu_{nm}(\omega)|^2\}. \tag{37}$$

According to Corollary 1, $E\{|\nu_{nm}(\omega)|^2\} = \sigma_0^2$. Therefore, we can rewrite (37) as

$$E\{|\Psi_{nm}(R,\omega)|^2\} = E\{|\alpha_{nm}(\omega)|^2\} |j_n\left(\frac{\omega}{c}R\right)|^2 + \sigma_0^2. \tag{38}$$

From this, signal to noise ratio (SNR) for the $(m,n)^{th}$ mode at frequency ω is

$$(SNR)_{nm}(\omega) = \frac{E\{|\alpha_{nm}(\omega)|^2\}|j_n\left(\frac{\omega}{c}R\right)|^2}{\sigma_0^2} \tag{39}$$

$$\leq (SNR)_{\alpha,\max}|j_n\left(\frac{\omega}{c}R\right)|^2 \tag{40}$$

where (40) follows from (16) and (17).

Next, based on the properties of the Bessel functions [41, p. 362] and the spherical Bessel functions [41, p. 437] and following a few intermediate steps, we can derive the following bound for the spherical Bessel functions for large n

$$|j_n(z)| \leq \frac{\sqrt{\pi}}{2}\left(\frac{z}{2}\right)^n \frac{1}{\Gamma(n+3/2)}, \quad z \geq 0 \tag{41}$$

where $\Gamma(\cdot)$ is the Gamma function. Therefore,

$$(SNR)_{nm}(\omega)<(SNR)_{\alpha,\max}\frac{e}{2(2n+1)^2}\left(\frac{e\omega R/c}{2n+1}\right)^{2n}. \tag{42}$$

This result is obtained using the Stirling lower bound for the Gamma functions

$$\Gamma(n+3/2) > \sqrt{2\pi e}\left(\frac{n+1/2}{e}\right)^{n+1}. \tag{43}$$

Now, using the exponential inequality, $(1+x/n)^n \leq e^x$ for $n \neq 0$, we rewrite (42) as

$$(SNR)_{nm}(\omega) \leq (SNR)_{\alpha,\max}\beta e^{(e\omega R/c-2n)}, \tag{44}$$

where $\beta = 2en^2/(2n+1)^4$. Since $\beta < 1$, for $n > 0$, we have

$$(SNR)_{nm}(\omega) < (SNR)_{\alpha,\max}e^{(e\omega R/c-2n)}. \tag{45}$$

Note that at the $(m,n)^{th}$ mode, it is not possible to detect signals within the band of frequencies where the SNR drops below a certain threshold γ. Hence, for a frequency to be usable to capture information at the $(m,n)^{th}$ mode, the SNR must be larger than or equal to the threshold γ. The frequency at which the $(SNR)_{n,m}(\omega)$ is at least equal to the threshold γ is the critical frequency F_n (where $\omega_n = 2\pi F_n$). Therefore,

$$(SNR)_{\alpha,\max}e^{(2\pi eF_nR/c-2n)} = \gamma. \tag{46}$$

This result is easily derived based on the reasoning provided in Section III-B. Here, we briefly discuss the reasoning: as depicted in Fig. 1, expect for the 0^{th} order, spherical Bessel functions show a high pass characteristics. As a result, for frequencies less then a critical frequency F_n, the magnitude of the n^{th} $(n > 0)$ order spherical Bessel function is negligible. Therefore, at each spatial mode $n > 0$, for

frequencies less than the critical frequency F_n, it is not possible to maintain the SNR at least equal to the threshold γ.

Now, making F_n the subject of the formula in (46) yields (15). This means that for spatial modes $n > 0$, signals below frequency F_n (15) are not detectable since (46) will not be satisfied. Observe that for any particular mode $n(> 0)$, if $F_n > F_0 - W$, the effective bandwidth of that mode is $F_0 + W - F_n$. In addition, if $F_n > F_0 + W$, the effective bandwidth of this mode and modes above this is zero. It should also be noted that for a fixed value of radius, $j_0(z)$ is active within the frequency range $[0, \infty)$ as depicted in Fig 1, hence, effective bandwidth of the 0^{th} mode is $2W$. These arguments are written mathematically as (14). ■

APPENDIX C
PROOF OF THE ORTHOGONALITY OF THE FUNCTIONS $\phi_\ell(t)$

Proof: Since

$$\phi_\ell(t) = e^{j2\pi W_{0n}(t-\frac{\ell}{W_n})}\frac{\sin \pi W_n(t-\frac{\ell}{W_n})}{\pi W_n(t-\frac{\ell}{W_n})}, \tag{47}$$

$$\begin{aligned}\int_{-\infty}^{\infty}\phi_\ell(t)\phi^*_{\ell'}(t)dt &= \int_{-\infty}^{\infty} e^{j2\pi W_{0n}(t-\frac{\ell}{W_n})}\frac{\sin \pi W_n(t-\frac{\ell}{W_n})}{\pi W_n(t-\frac{\ell}{W_n})} e^{-j2\pi W_{0n}(t-\frac{\ell'}{W_n})}\frac{\sin \pi W_n(t-\frac{\ell'}{W_n})}{\pi W_n(t-\frac{\ell'}{W_n})}dt \\ &= \kappa\int_{-\infty}^{\infty}\frac{\sin \pi W_n(t-\frac{\ell}{W_n})}{\pi W_n(t-\frac{\ell}{W_n})}\frac{\sin \pi W_n(t-\frac{\ell'}{W_n})}{\pi W_n(t-\frac{\ell'}{W_n})}dt \\ &= \begin{cases} 0 & \ell \neq \ell' \\ \frac{1}{W_n} & \ell = \ell' \end{cases}\end{aligned} \tag{48}$$

where $\kappa = e^{-j2\pi(\ell-\ell')W_{0n}/W_n}$ and for $\ell = \ell'$, $\kappa = 1$. Here, (48) is derived using the fact that [24, eqn. 11]

$$\begin{aligned}&\int_{-\infty}^{\infty}\frac{\sin \pi W_n(t-\frac{\ell}{W_n})}{\pi W_n(t-\frac{\ell}{W_n})}\frac{\sin \pi W_n(t-\frac{\ell'}{W_n})}{\pi W_n(t-\frac{\ell'}{W_n})}dt \\ &= \begin{cases} 0 & \ell \neq \ell' \\ \frac{1}{W_n} & \ell = \ell'. \end{cases}\end{aligned} \tag{49}$$

Thus, the functions $\phi_\ell(t)$ are orthogonal over time. ■

APPENDIX D
PROOF OF THEOREM 4

Proof: We start from (27) and by expanding the sum, we obtain

$$D = \sum_{n=0}^{N_{\max}}(2n+1) + T_{eff}\sum_{n=0}^{N_{max}}(2n+1)W_n. \tag{50}$$

Substituting (7) and (14) in (50) yields

$$D = \sum_{n=0}^{N_{\max}} (2n+1) + 2W(T+\frac{2R}{c}) \sum_{n=0}^{N_{\min}} (2n+1) + (T+\frac{2R}{c}) \sum_{n>N_{\min}}^{N_{\max}} (2n+1)(F_0+W-F_n)$$
$$= D_1 + 2W(T+\frac{2R}{c})D_2 + (T+\frac{2R}{c})D_3 \quad (51)$$

considering,

$$D_1 = \sum_{n=0}^{N_{\max}} (2n+1), \quad (52)$$

$$D_2 = \sum_{n=0}^{N_{\min}} (2n+1) \quad (53)$$

and

$$D_3 = \sum_{n>N_{\min}}^{N_{\max}} (2n+1)(F_0+W-F_n). \quad (54)$$

Now, using the sum of the first p odd numbers, $\sum_{p=0}^{P}(2p+1) = (P+1)^2$, we can rewrite (52) and (53) as

$$D_1 = (N_{\max}+1)^2 \quad (55)$$

and

$$D_2 = (N_{\min}+1)^2. \quad (56)$$

Further, replacing F_n by (15) in (54) and following a few intermediate steps, we obtain

$$D_3 \leq 2W\Big[2\Big(e\pi\frac{R}{c}\Big)^2\Big(F_0W-\frac{1}{3}W^2\Big)+e\pi\frac{R}{c}(2F_0-W)+\log\Big(\frac{(SNR)_{\alpha,\max}}{\gamma}\Big)\Big(e\pi W\frac{R}{c}+1\Big)\Big]. \quad (57)$$

Finally, substituting (55), (56) and (57) in (51), we deduce the upper bound on the signal degrees of freedom (28). ■

REFERENCES

[1] A. Paulraj and C. Papadias, "Space-time processing for wireless communications," *IEEE Signal Processing Magazine*, vol. 14, no. 6, pp. 49–83, Nov. 1997.

[2] R. Kohno, "Spatial and temporal communication theory using adaptive antenna array," *IEEE Personal Communications*, vol. 5, no. 1, pp. 28–35, Feb. 1998.

[3] N. Yair and A. J. Goldsmith, "Exploiting spatial degrees of freedom in MIMO cognitive radio systems," in *IEEE International Conference on Communications (ICC)*, 2012, pp. 3499–3504.

[4] S. Hua, C. Geng, T. Gou, and S. A. Jafar, "Degrees of freedom of MIMO X networks: Spatial scale invariance, one-sided decomposability and linear feasibility," in *EEE International Symposium on Information Theory Proceedings (ISIT)*, 2012, pp. 2082–2086.

[5] A. Ozgur, O. Leveque, and D. Tse, "Spatial degrees of freedom of large distributed MIMO systems and wireless ad hoc networks," *IEEE Journal on Selected Areas in Communications*, vol. 31, no. 2, pp. 202–214, February 2013.

[6] I. E. Telatar, "Capacity of multi-antenna gaussian channels," *European Transactions on Telecommunications*, vol. 10, pp. 585–595, 1999.

[7] G. J. Foschini and M. J. Gans, "On limits of wireless communications in a fading environment when using multiple antennas," *Wireless Personal Communications*, vol. 6, pp. 311–335, 1998.

[8] P. D. Teal, T. D. Abhayapala, and R. A. Kennedy, "Spatial correlation for general distributions of scatterers," *IEEE Signal Processing Letters*, vol. 9, no. 10, pp. 305–308, Oct. 2002.

[9] A. M. Sayeed, "Deconstructing multiantenna fading channels," *IEEE Transactions on Signal Processing*, vol. 50, no. 10, pp. 2563 – 2579, Oct. 2002.

[10] K. Liu, V. Raghavan, and A. Sayeed, "Capacity scaling and spectral efficiency in wideband correlated MIMO channels," *IEEE Transactions on Information Theory*, pp. 2504–2526, Oct. 2003.

[11] D. A. B. Miller, "Communicating with waves between volumes: evaluating orthogonal spatial channels and limits on coupling strengths," *Applied Optics*, vol. 39, no. 11, pp. 1681–1699, Aprill 2000.

[12] T. S. Pollock, T. D. Abhayapala, and R. A. Kennedy, "Antenna saturation effects on MIMO capacity," in *Proc. International Conference on Communications, ICC'03*, vol. 3, May 2003, pp. 2301–2305.

[13] L. Hanlen and M. Fu, "Wireless communication systems with spatial diversity: a volumetric model," *IEEE Transactions On Wireless Communications*, vol. 5, no. 1, pp. 133–142, Jan. 2006.

[14] R. A. Kennedy, T. D. Abhayapala, and H. M. Jones, "Bounds on the spatial richness of multipath," in *Australian Communications Theory Workshop, AusCTW*, Canberra,Austraia, Feb. 4-5 2002, pp. 76–80.

[15] R. A. Kennedy, P. Sadeghi, T. D. Abhayapala, and H. M. Jones, "Intrinsic limits of dimensionality and richness in random multipath fields," *IEEE Transactions on Signal processing*, vol. 55, no. 6, pp. 2542–2556, June 2007.

[16] A. S. Y. Poon, R. W. Brodersen, and D. N. C. Tse, "Degrees of freedom in multiple-antenna channels: A signal space approach," *IEEE Transactions on Information Theory*, vol. 51, no. 2, pp. 523–536, Feb. 2005.

[17] M. Franceschetti, "On the information content of scattered waves," in *IEEE International Symposium on Information Theory Proceedings*, 2012, pp. 1523–1527.

[18] M. Franceschetti and K. Chakraborty, "Space-time duality in multiple antenna channels," *IEEE Transactions on Wireless Communications*, vol. 8, no. 4, pp. 1733–1743, April 2009.

[19] D. Colton and R. Kress, *Inverse acoustic and electromagnetic scattering theory, Applied Mathematical Sciences*, 2nd ed., 1998, vol. 93.

[20] L. W. Hanlen and T. D. Abhayapala, "Bounds on space-time-frequency dimensionality," in *Australian Communications Theory Workshop, AusCTW*, Adelaide, Austraia, Feb. 5-8 2007, pp. 144–149.

[21] ——, "Space-time-frequency degrees of freedom: Fundamental limits for spatial information," in *IEEE Intl.Symp. on Information Theory 2007, ISIT 2007*, Nice, France, June 24-29 2007, pp. 701–705.

[22] F. Bashar, S. A. Salehin, and T. D. Abhayapala, "Analysis of degrees of freedom of wideband random multipath fields observed over time and space windows," in *IEEE Statistical Signal Processing Workshop*, Gold Coast, Australia, 29 Jun - 02 Jul 2014, accepted.

[23] F. Bashar and T. D. Abhayapala, "Degrees of freedom of band limited signals measured over space," in *The 12th International Symposium on Communications and Information Technologies (ISCIT 2012)*, 2012, pp. 735 –740.

[24] C. E. Shannon, "Communication in the presence of noise," *Proceedings of the IRE*, vol. 37, no. 1, pp. 10–21, Jan. 1949, reprinted in Proceedings of the IEEE, vol. 86, no. 2, pp. 447-457, Feb. 1998.

[25] D. Slepian and H. O. Pollak, "Prolate spheroidal wave functions, Fourier analysis and uncertainty - i," *Bell System Technical Journal*, pp. 43–64, January 1961.

[26] J. H. Landau and O. H. Pollak, "Prolate spheroidal wave functions, Fourier analysis and uncertainty - ii," *Bell System Technical Journal*, vol. 40, pp. 65–84, January 1961.

[27] ——, "Prolate spheroidal wave functions, Fourier analysis and uncertainty - iii: The dimension of the space of essentially time- and band-limited signals," *Bell System Technical Journal*, vol. 41, pp. 1295–1336, July 1962.

[28] D. Slepian, "Some comments on fourier analysis, uncertainty and modeling," *SIAM Review*, vol. 25, pp. 379–393, 1983.

[29] P. M. Dollard, "On the time-bandwidth concentration of signal functions forming given geometric vector configurations," *IEEE Transactions on Information Theory*, vol. 10, no. 4, pp. 328–338, Oct. 1964.

[30] R. S. Bennett, "The intrinsic dimensionality of signal collections," *IEEE Transactions on Information Theory*, vol. 15, no. 5, pp. 517–525, Sept. 1969.

[31] A. J. Jerri, "The shannon sampling theorem-its various extensions and applications: A tutorial review," *Proceedings of the IEEE*, vol. 65, no. 11, pp. 1565–1595, Nov. 1977.

[32] G. B. Arfken and H. J. Weber, *Mathematical Methods for Physicists*, 6th ed. Elsevier Academic Press, 2005.

[33] A. Bostrom, G. Kristensson, and S. Strom, *Transformation properties of plane spherical and cylindrical scalar & vector wave functions*. Elsevier Science Publishers, 1991, ch. 4, pp. 165–210.

[34] E. G. Williams, *Fourier Acoustics: Sound Radiation and Nearfield Acoustical Holography*. New York: Academic Press, 1999.

[35] R. G. Gallager, *Information Theory and Reliable Communication*. New York, USA: John Wiley & Sons, 1968.

[36] J. Krolik and D. Swingler, "Multiple broad-band source location using steered covariance matrices," *IEEE Transactions on Acoustics, Speech and Signal Processing*, vol. 37, no. 10, pp. 1481 – 1494, Oct. 1989.

[37] A. El-Keyi and B. Champagne, "Cooperative mimo-beamforming for multiuser relay networks," in *IEEE International Conference on Acoustics, Speech and Signal Processing, 2008, ICASSP 2008*, March 2008, pp. 2749–2752.

[38] K. Gomadam, V. R. Cadambe, and S. A. Jafar, "A distributed numerical approach to interference alignment and applications to wireless interference networks," *IEEE Transactions on Information Theory*, vol. 57, no. 6, pp. 3309–3322, June 2011.

[39] A. Ozgur, O. Leveque, and D. Tse, "Hierarchical cooperation achieves optimal capacity scaling in ad-hoc networks," *IEEE Transactions on Information Theory*, vol. 53, pp. 3549–3572, 2007.

[40] M. Franceschetti, M. D. Migliore, and P. Minero, "The capacity of wireless networks: Information-theoretic and physical limits," *IEEE Transactions on Information Theory*, vol. 55, no. 8, pp. 3413–3424, August 2009.

[41] M. Abramowitz and I. A. Stegun, Eds., *Handbook of Mathematical Functions*, 10th ed., National Bureau of Standards, US Government Printing Office, Washington, DC, 1972, vol. 55.